

# Modelling of Photovoltaic Modules Optical Losses Due to Saharan Dust Deposition in Dakar, Senegal, West Africa

Dialo Diop<sup>1</sup>, Mamadou Simina Drame<sup>1,2</sup>, Moussa Diallo<sup>3</sup>, David Malec<sup>4\*</sup>, Dominique Mary<sup>4</sup>, Philippe Guillot<sup>5</sup>

<sup>1</sup>Groupe des Laboratoires de Physique des Solides des Sciences des Matériaux (GLPSSM), Département de Physique, Faculté des Sciences et Techniques (FST), Université Cheikh Anta Diop, Dakar, Sénégal

<sup>2</sup>Laboratoire de Physique de l'Atmosphère et de l'Océan Siméon Fongang, Université Cheikh Anta Diop, Dakar, Sénégal

<sup>3</sup>Department of Computer Science, Polytechnic Institute (ESP), Université Cheikh Anta Diop, Dakar, Sénégal

<sup>4</sup>Laboratoire Plasma et Conversion d'Énergie (LAPLACE), Université de Toulouse, UPS, INPT, CNRS, Toulouse, France

<sup>5</sup>Equipe Diagnostics de Plasmas Hors Equilibre (DPHE), Université de Toulouse, INU Champollion, Albi, France

Email: \*david.malec@laplace.univ-tlse.fr

**How to cite this paper:** Diop, D., Drame, M.S., Diallo, M., Malec, D., Mary, D. and Guillot, P. (2020) Modelling of Photovoltaic Modules Optical Losses Due to Saharan Dust Deposition in Dakar, Senegal, West Africa. *Smart Grid and Renewable Energy*, 11, 89-102.

<https://doi.org/10.4236/sgre.2020.117007>

**Received:** June 17, 2020

**Accepted:** July 28, 2020

**Published:** July 31, 2020

Copyright © 2020 by author(s) and Scientific Research Publishing Inc. This work is licensed under the Creative Commons Attribution International License (CC BY 4.0).

<http://creativecommons.org/licenses/by/4.0/>



Open Access

---

## Abstract

This study aims to evaluate the optical losses of photovoltaic modules due to Saharan dust deposition in Dakar, Senegal, West Africa. For this purpose, an air-dust-glass system is modeled to simulate optical losses in transmittance and reflectance. To do this, we have collected dust samples from Photo-Voltaic (PV) surface in Dakar area (14°42'N latitude, 17°28'W longitude), Senegal. X-ray fluorescence reveals that silicon (Si), iron (Fe), calcium (Ca) and potassium (K) mainly composed these dust samples. Then, dust refractive indices obtained from an ellipsometer were used as an input to be used in the model. Simulations show that for radiation (at normal incidence) arriving on a dust layer of 30 μm-thick (corresponding to a dust deposit of 1.63 g/m<sup>2</sup>), 79% of the visible spectrum is transmitted; 19% is reflected and 2% is absorbed. Overall, the transmittance decreases by more than 50% as of dust layer of 70 μm-thick corresponding to a dust deposit of 3.3 g/m<sup>2</sup>.

## Keywords

Dust Characterization, Modeling, Ellipsometry, PV Transmittance, Solar Panel, Spin Coating, X-Ray Fluorescence

---

## 1. Study Context

Recently, a great deal of effort has been made to increase the production of solar

energy worldwide. In 2016, the International Energy Agency (IEA) [1] affirmed that approximately 315 GW of photovoltaic power was installed worldwide. On the other hand, the projections for 2017 and 2022 were 385 GW and 500 GW respectively [2]. In Africa, solar production is expected to reach 70 GW by 2030 [3]. Since 2015, Senegal has increased its solar capacity with the installation of new plants according to Aidara *et al.* [4]. However, the efficiency of PV module production in arid and semi-arid regions is strongly influenced by dust deposition [5]. For example, Darwish *et al.* [6] studied 15 types of dust and concluded that six of them (ash, calcium, limestone, soil, sand and silica) significantly reduce the PV modules efficiency. Similarly, results based on theoretical models have shown the effect of dust deposition by considering three types of dust: red earth, limestone and ash. These works show that the performance of PV is highly dependent on both composition and source of these particles [7]. Indeed, the nature of the dust is one of main causes of arriving radiation attenuation on PV modules surface (Qasem *et al.* [8], Makkar *et al.* [9], Mackey *et al.* [10]). Other studies carried out in Asia have shown the importance of taking into account dust deposits on photovoltaic installations (Nahar and Gupta [11], Hasan and Sayigh [12], Gürtürk *et al.* [13], El-Shobokshy and Hussein [14], Javed *et al.* [15], Paudyal *et al.* [16], Zarei and Abdolzadeh [17], Guo and Pan [18]). Consequently, dust deposition effect on yields of photovoltaic cells has been highlighted by experimental methods (Mani and Pillai [19]) but also by empirical calculations (Hegazy *et al.* [20]).

In south Sahara, initial studies have shown that dust reduces the efficiency of solar panels (Ndiaye *et al.* [21], Ansmann *et al.* [22], Rao *et al.* [23], Saidan *et al.* [24]). Moreover, this region is the world largest source of dust according to Marticorena *et al.* [25].

However, these kinds of experimental studies are still limited in West Africa, particularly in Senegal. This is due to the lack of technical devices to carry out the characterizations but also to determine optical properties such as transmittance, reflectance and absorbance. Indeed, the data obtained through characterization techniques will make it possible to know the source, the optical properties and the composition of the dust. This study characterizes the dust samples collected in Dakar and also evaluates the transmission and reflection losses of the air-dust-glass system.

The paper is subdivided into three parts. The first part presents the experimental (characterization techniques) and theoretical (modeling) approaches. Then, the second part presents the results of dust characterization and the simulations resulting from the modeling of the losses in transmittance and reflectance of solar radiation. Finally, the last section draws the main conclusions of this work.

## 2. Material and Methods

### 2.1. Experimental Approach

In this work, we collect samples directly from PV surfaces in Dakar (14°44'N la-

titude and 17°27'28"W longitude). These samples are collected in vials as shown in **Figure 1(b)**. The samples are then analyzed by X-ray fluorescence (EDXRF) to determine the different chemical elements. The instrument used to determine these elementary compositions is a Horiba Jobin Yvon XGT-5000. It is equipped with a tungsten X-ray tube, a beryllium window and a high-purity Si detector; it operates at 50 kV-max/1mA-max. Next, thin layers of dust are made on glass plates (see **Figure 1(c)**) with a spin coater according to the spin coating technique using an isopropanol solution as described by Lawrence *et al.* [26]. A digital microscope (Keyence, VHX1000) with a magnification of 100 - 1000 nm or 500 - 5000 nm is used to determine the thickness of dust layer. In addition, a SOPRA GES-5 type ellipsometer with a spectral ranging from 190 to 2500 nm is used to obtain real and imaginary dust indices (Pristinski *et al.* [27]). These optical indices obtained from the ellipsometer are used as input parameters for the proposed model. To ensure the reliability of the ellipsometer results, refractions index are compared with those measured by the AERONET sunphotometer stationed in Dakar (Holben *et al.* [28]). Indeed, the same particles measured by the sunphotometer were deposited on PV modules surface in Dakar. And finally, UV-Visible spectrophotometer is used to validate the model.

## 2.2. Theoretical Approach

The approach consists of simulating an electromagnetic wave with oblique or normal incidence on dust layer deposited on glass as shown in **Figure 2**. Electromagnetic wave passes through a multilayer optical system (Air-Dust-Glass). This wave can be reflected, transmitted or partially absorbed at each interface by the different constituents of the layers. Air and glass are characterized by their refractive index:  $n_0$  and  $n_2$  respectively. The dust is characterized by its optical index ( $n_1$ ) which varies as a function of wavelength according to Equations (1) and (2) described by Bashara and Azzam [29].

$$n_1(\lambda) = n(\lambda) - ik(\lambda) \quad (1)$$

$$k = \frac{\lambda}{4\pi} \alpha(\lambda) \quad (2)$$

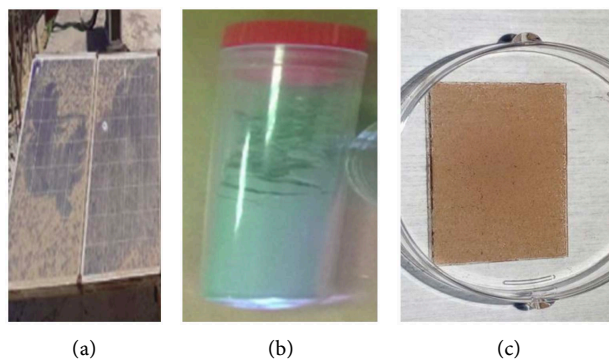


**Figure 1.** (a) Accumulation of dust on PV installed in Senegal; (b) Dust samples collected and (c) Thin layer of dust deposited on glass with a spin coater.

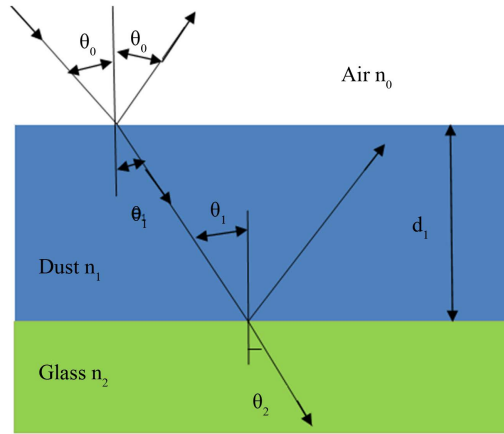


**Figure 2.** Conceptual diagram of the proposed model with its different layers (air-dust-glass).

$n$ ,  $k$ ,  $\alpha$  and  $\lambda$  respectively represent the refractive index (real index) of dust, the dust extinction coefficient (imaginary index), the dust absorption coefficient and the solar radiation wavelength. Next, we calculate the Fresnel reflection and transmission coefficients at the layer interfaces for  $p$  and  $s$  polarization by applying electric  $E$  and magnetic  $B$  field conservation and Descartes' formulas as described by Mahdjoub *et al.* [30], Berthier and Lafait [31]. We use the equations of Macleod [32], Born and Wolf [33] and McCrackin *et al.* [34]:

For the air-dust interface:

$$n_0 \sin \Theta_0 = n_1 \sin \Theta_1 \tag{3}$$

And for the dust-glass interface the equation becomes:

$$n_1 \sin \Theta_1 = n_2 \sin \Theta_2 \tag{4}$$

$$\beta = 2\pi \cdot n_1 \cos \Theta_1 \left( \frac{d_1}{\lambda} \right) \tag{5}$$

where  $\beta$  is the phase difference introduced by the reflection and  $d_1$  is the dust layer thickness. The overall reflection ( $r_p$ ,  $r_s$ ) and transmission ( $t_p$ ,  $t_s$ ) coefficients of the system for a  $p$  or  $s$  polarization are shown in the equations below:

$$r_p = \frac{r_{01}^p + r_{12}^p \exp(-2i\beta)}{1 + r_{01}^p r_{12}^p \exp(-2i\beta)} \tag{6}$$

$$r_s = \frac{r_{01}^s + r_{12}^s \exp(-2i\beta)}{1 + r_{01}^s r_{12}^s \exp(-2i\beta)} \tag{7}$$

$$t_s = \frac{t_{01}^s t_{12}^s \exp(-i\beta)}{1 + r_{01}^s r_{12}^s \exp(-2i\beta)} \tag{8}$$

$$t_p = \frac{t_{01}^p t_{12}^p \exp(-i\beta)}{1 + r_{01}^p r_{12}^p \exp(-2i\beta)} \tag{9}$$

$$T_p = |t_p t_p| \frac{n_2 \cos \Theta_2}{n_0 \cos \Theta_0} \tag{10}$$

$$T_s = |t_s t_s| \frac{n_2 \cos \Theta_2}{n_0 \cos \Theta_0} \tag{11}$$

$T_s$ ,  $T_p$  are Transmittances for  $s$  and  $p$  polarization.

$$R_p = |r_p r_p| \quad (12)$$

$$R_s = |r_s r_s| \quad (13)$$

$R_s$  and  $R_p$  are reflectances for  $s$  and  $p$  polarization.

$$T = \frac{T_s + T_p}{2} \quad (14)$$

$$R = \frac{R_s + R_p}{2} \quad (15)$$

$$A = 100 - (R + T) \quad (16)$$

$T$ ,  $R$  and  $A$  are the mean reflectance, mean transmittance and absorbance of the system, respectively.

### 3. Results and Discussions

#### 3.1. X-Ray Fluorescence (XRF) Analysis of Dust Samples

**Figure 3** shows the dust samples elemental analysis by X-ray fluorescence (XRF). It indicates that the dust is dominated by elements such as: Si, Fe, Ca, K, Ti, P, S, Zn, Mn, Zr. Some elements such as Cr, Cd, Br, Pb, Cu and Hg are minority or trace elements.

**Figure 4** shows the detected element mass concentration in Dakar dust. It determines the mass proportions of each chemical element. The analysis reveals that this powder is mainly composed of Silicon (Si) with a rate of more than 50.1% of the total mass. The remainder consists of 16.8% of Fe, 10.6% of Ca, 1.5% of K, 1.4% of Ti, 0.98% of P and 0.5% of S. Trace elements such as Cu, Zn, Sr, Zr were also detected. However, X-ray fluorescence diffraction (XRF) does not detect very light elements such as aluminum.

These two materials are used as reference and validation elements to determine the concentrations of sand elements. We find the same chemical elements for these three samples, which proves that the dust collected in Dakar is of sandy nature. However, main elements such as Si, Ca, Fe, S and P are more important in mass in Saharan dust rather than the other samples (**Figure 5**).

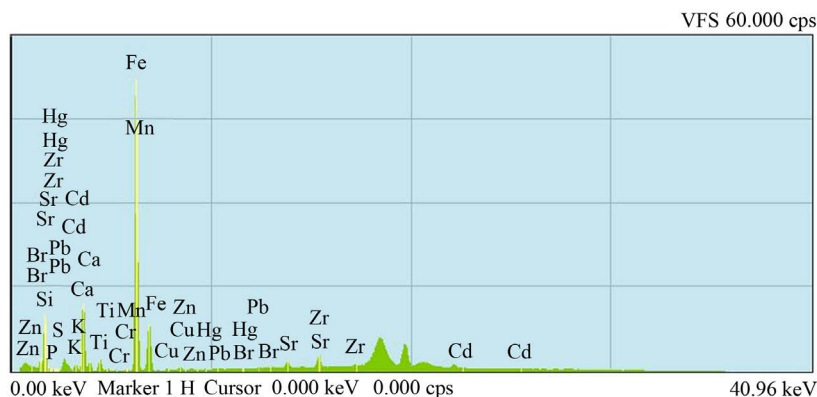


**Figure 3.** Chemical elements detected in Dakar dust.

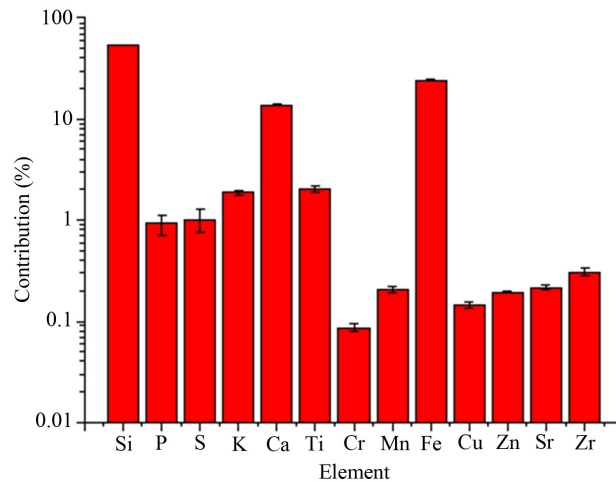


**Figure 4.** Mass percentage of elements detected in Dakar dust.

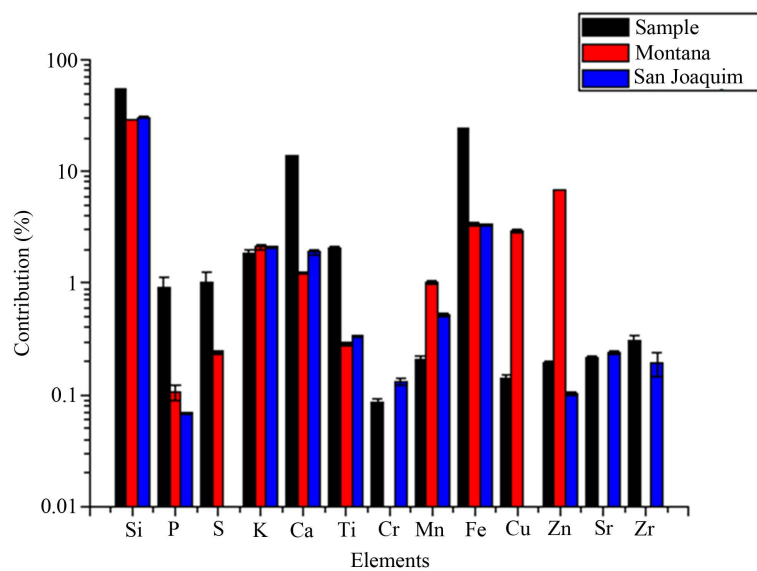


**Figure 5.** Comparison between Dakar dust (in black) and two standardized and certified reference sand samples named SRM-2709a and SRM-2710 respectively of San Joaquin (in blue) and Montana (in red) in USA.

## 3.2. Model Validation

### 3.2.1. Optical Index Validation

The model developed uses real and imaginary refractive indices as input parameters. Consequently, the indices of the dust samples collected in Dakar were obtained from an ellipsometer. To validate the ellipsometer data, the refractive indices are compared with those measured by AERONET sunphotometer stationed in Dakar. Indeed, we use AERONET data corresponding to the same periods. **Figure 6** shows a comparison between the dust real (**Figure 6** left) and imaginary (**Figure 6** right) indices obtained from the ellipsometer and the sunphotometer. Firstly, it clearly shows that the same atmospheric particles over Dakar were deposited on solar panels surface. The curves are in good agreement especially in the visible spectrum.

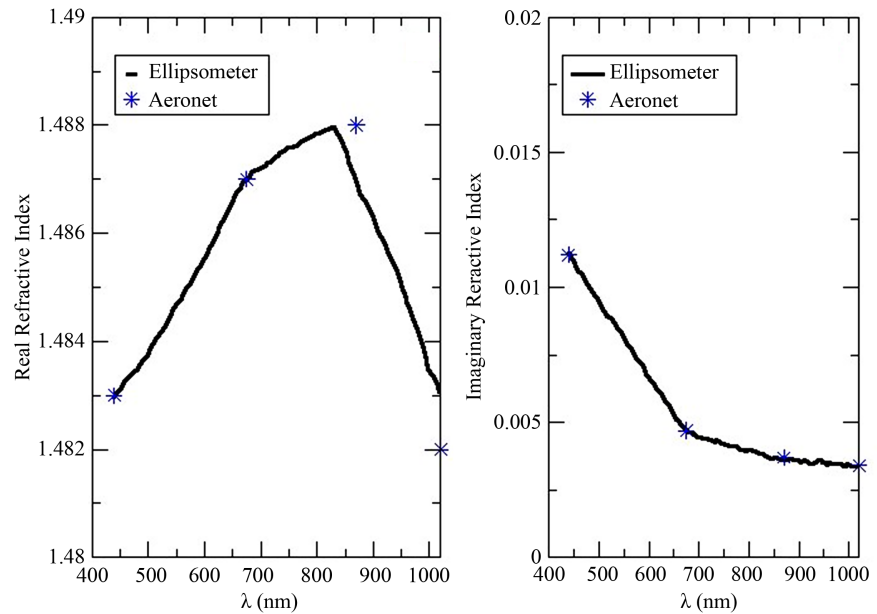


**Figure 6.** Validation of ellipsometer refractive indices by atmospheric data from the AERONET sunphotometer. Comparison between real indices (left) and imaginary indices (right).

From the indices obtained, we will now simulate the losses in transmittance and reflectance of solar radiation.

### 3.2.2. Transmittance Validation

To validate the model outputs, a comparison with experimental measurements from a UV-visible spectrophotometer was conducted. Indeed, electromagnetic radiation is sent by an UV-visible spectrophotometer over a thin layer of dust 35  $\mu\text{m}$ -thick (corresponding to a deposit of 1.63  $\text{g}/\text{m}^2$ ) deposited on a glass substrate. Then we compare the measured and simulated transmittance. **Figure 7** illustrates this comparison between these two transmittances (simulated in red and measured in black) and that of clean glass in cyan color. First of all, the results show that a thin layer of dust of 35  $\mu\text{m}$  lets through (transmittance) on average 75% of solar radiation, which corresponds to a loss of almost 21% compared to clean glass. Then the comparison shows a good agreement between the transmittances measured by the spectrophotometer and simulated by the model especially in the visible range between 450 and 800 nm. The correlation coefficient between these two curves is more than 88%.

### 3.3. Solar Radiation Transmittance Losses

In this section, we perform the model sensitivity studies and then assess the impact of dust on radiation components.

The first step is to simulate the influence of dust layers on solar radiation transmission (transmittance) through an air-dust-glass system. For this purpose, the model is executed with different layer sizes. **Figure 8** shows the transmittance for an air-dust-glass system for different dust layer sizes. These values are

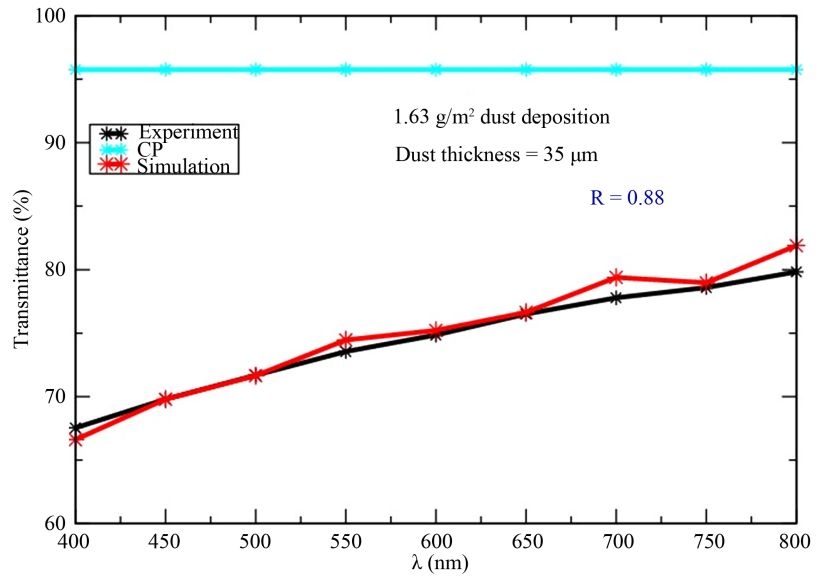


**Figure 7.** Comparison between the transmittance measured by the spectrophotometer (in black) and simulated by the model (in red) for a dust layer of 35  $\mu\text{m}$ . The cyan curve represents the transmittance of clean glass.

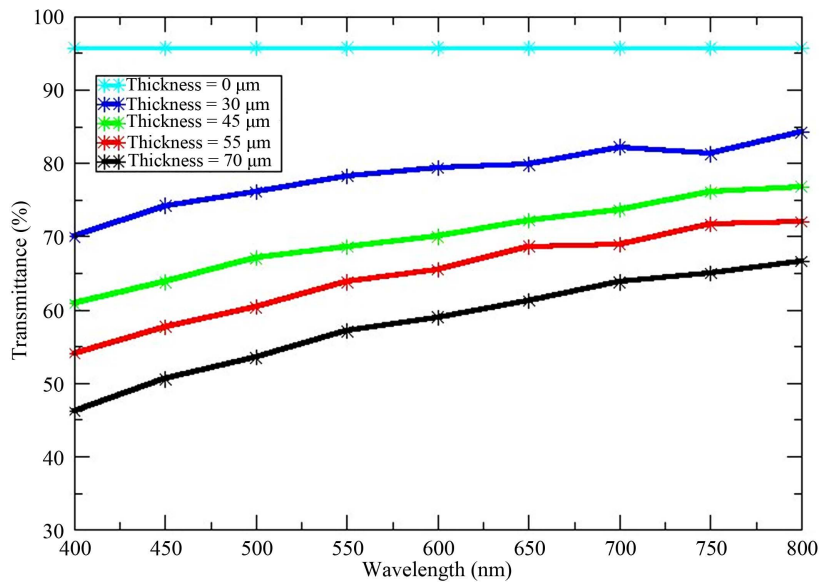


**Figure 8.** Simulations of transmittances as a function of wavelength for different dust layers with thickness of 30, 45, 55 and 70  $\mu\text{m}$ .

30  $\mu\text{m}$  (corresponding to a dust deposit of 1.4  $\text{g}/\text{m}^2$ ), 45  $\mu\text{m}$  (corresponding to a dust deposit of 2.1  $\text{g}/\text{m}^2$ ), 55  $\mu\text{m}$  (corresponding to a dust deposit of 2.6  $\text{g}/\text{m}^2$ ) and 70  $\mu\text{m}$  (corresponding to a dust deposit of 3.3  $\text{g}/\text{m}^2$ ) respectively.

The correspondence between layer size in  $\mu\text{m}$  and dust deposition in  $\text{g}/\text{m}^2$  is made by considering a dust density about 2.6  $\text{g}/\text{cm}^3$  according to Ansmann *et al.* [22]. The cyan curve in **Figure 8** corresponds to the transmittance for clean glass (without dust), which is considered as absolute reference. Overall, a clean glass allows all the radiation to pass through with a transmittance of around 95%.

Next, **Figure 8** shows that a dust deposit of  $1.4 \text{ g/m}^2$  (corresponding to a layer size of  $30 \text{ }\mu\text{m}$ ) causes 18% loss of transmittance. Then, we note that the transmittance decreases inversely with the layer thickness. Indeed, for thickness of 45, 55 and  $70 \text{ }\mu\text{m}$ , the mean transmittance is of 70%, 64.7% and 58% respectively. Overall, the results show that the transmittances decrease in short wavelengths. This is due to the Mie scattering of these particles (Xie *et al.* [35]). These results are in good agreement with those of Yun-Yun and Zhang [36]. However, these losses are greater than those found by Mastekbayeva and Kumar [37]. They showed that for a period of 30 days and for  $3.72 \text{ g/m}^2$  of dust deposition, transmission losses were about 24.2%. These differences are due to the nature of the dusts considered. In summary, half of the radiation is lost when the dust layer thickness reaches  $70 \text{ }\mu\text{m}$ . This radiation is blocked by dust, as shown by Hegazy *et al.* [20].

### 3.4. Solar Reflectance Losses

**Figure 9** shows the reflectance losses (of the air-dust-glass system) for different dust layers considered in the model. Indeed, this figure represents the reflectance as a function of wavelength for four dust layer thicknesses ( $30, 45, 55$  and  $70 \text{ }\mu\text{m}$ ). Overall, we note that the average reflectance increases from 26% to 53% if the layer thickness increases from  $30$  to  $70 \text{ }\mu\text{m}$ .

Reflectance is more important for short wavelengths between  $400$  and  $600 \text{ nm}$ . According to Kaufman *et al.* [38], the high reflectance at wavelengths  $462 - 500 \text{ nm}$  is due to the presence of iron atoms in the dust. Other studies such as that of Müller *et al.* [39] confirm these radiative properties of Saharan dust.

**Figure 10** shows the transmission losses as a function of different dust layers with thicknesses ranging from  $0$  to  $70 \text{ }\mu\text{m}$ . We note that the transmittance decreases as the thickness of the dust layer increases. These results are in good agreement

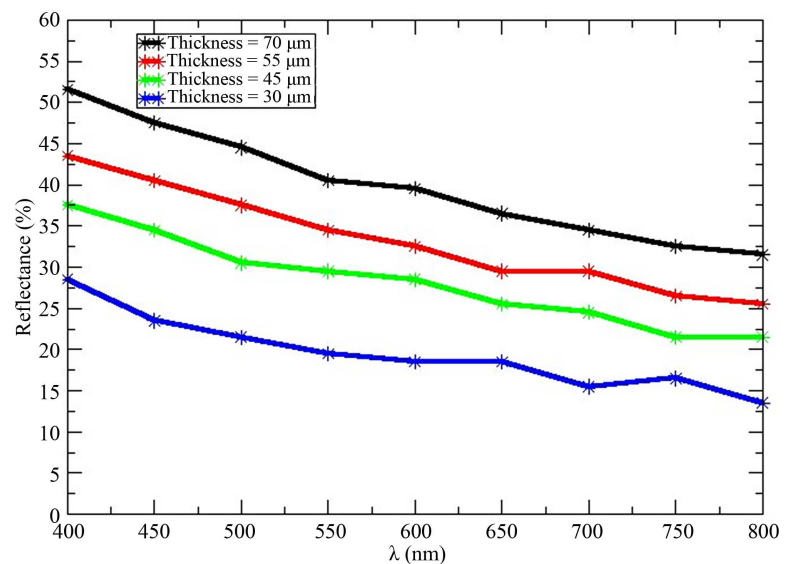


**Figure 9.** Simulations of reflectances as a function of wavelength for different dust layers with thickness of  $30, 45, 55$  and  $70 \text{ }\mu\text{m}$ .

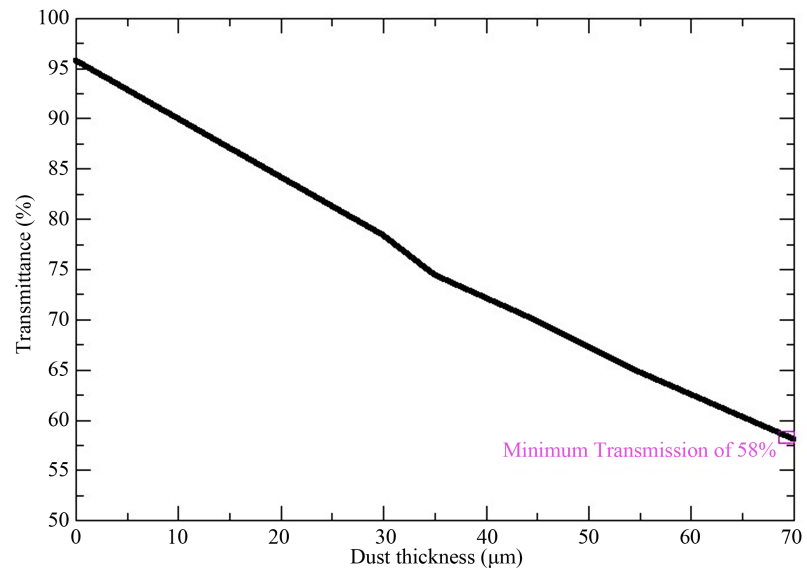


**Figure 10.** Simulation of transmission losses for dust layers (thickness ranging from 0 to 70 μm).

with those of Said and Walwil [40], Al-Hasan [41], Ebert and Bhushan [42], Dull *et al.* [43], Chaouki *et al.* [44] who showed the negative impact of dust layers on transmittances. Thus, this figure shows that the transmittance of solar radiation of a clean glass compared to an unclean glass could decrease by up to 58% for a layer of 70 μm.

#### 4. Conclusion

This work investigated the optical losses of solar radiation caused by dust deposition on solar panels surface. The objective was to characterize the dust collected on PV surface in Dakar (Senegal) and then to evaluate the impact of this dust layer on solar radiation. Firstly, the experimental study showed that Dakar dust is composed of 50.1% Si, 16.8% Fe, 10.6% Ca, 1.5% K, 1.4% Ti, 0.98% P, 0.5% S and the rest is traces such as Cu, Zn, Sr. An ellipsometer was used to obtain the dust refractive indices which will serve as input for the model. The model implemented was validated by transmittance measurements obtained with a UV-visible spectrophotometer. And secondly, simulations reveal that transmittance is reduced by half for dust layer about 70 μm (corresponding to a dust deposit of 3.3 g/m<sup>2</sup>).

#### Acknowledgements

The authors would like to thank Benoît Lantin, Benoit Schelgel and Pierre Hernandez from LAPLACE CARMAT Platform.

#### Conflicts of Interest

The authors declare no conflicts of interest regarding the publication of this paper.

## References

- [1] International Energy Agency (IEA) (2016) Photovoltaic Power System (PVPS) 2016 Snapshot of Global Photovoltaic Market. Technical Report.
- [2] International Energy Agency (IEA) (2017) Photovoltaic Power System (PVPS) Trends 2017 in Photovoltaic Applications-Executive Summary. Technical Report.
- [3] International Renewable Energy Agency (IRENA) (2016) Solar PV in Africa: Costs and Markets. Technical Report.
- [4] Aidara, M.C., Ndiaye, M.L. and Nkouna, W.M. (2018) Correlation between Dirt on the Photovoltaic Module Surface and Climatic Parameters in the Dakar Region, Senegal. 2018 7<sup>th</sup> International Conference on Renewable Energy Research and Applications (ICRERA), Paris, 14-17 October 2018, 517-521. <https://doi.org/10.1109/ICRERA.2018.8566807>
- [5] Dajuma, A., Yahaya, S., Touré, S., Diedhiou, A., Adamou, R., Konaré, A., Sido, M. and Golba, M. (2016) Sensitivity of Solar Photovoltaic Panel Efficiency to Weather and Dust over West Africa: Comparative Experimental Study between Niamey (Niger) and Abidjan (Côte d'Ivoire). *Computational Water, Energy, and Environmental Engineering*, **5**, 123-147. <https://doi.org/10.4236/cweee.2016.54012>
- [6] Darwish, Z.A., Kazem, H.A., Sopian, K., Al-Goul, M. and Alawadhi, H. (2015) Effect of Dust Pollutant Type on Photovoltaic Performance. *Renewable and Sustainable Energy Reviews*, **41**, 735-744. <https://doi.org/10.1016/j.rser.2014.08.068>
- [7] Kaldellis, J.K. and Kapsali, M. (2011) Simulating the Dust Effect on the Energy Performance of Photovoltaic Generators Based on Experimental Measurements. *Energy*, **36**, 5154-5161. <https://doi.org/10.1016/j.energy.2011.06.018>
- [8] Qasem, H., Betts, T.R., Müllejans, H., AlBusairi, H. and Gottschalg, R. (2014) Dust-Induced Shading on Photovoltaic Modules. *Progress in Photovoltaics: Research and Applications*, **22**, 218-226. <https://doi.org/10.1002/pip.2230>
- [9] Makkar, A., Raheja, A., Chawla, R. and Gupta, S. (2019) IoT Based Framework: Mathematical Modelling and Analysis of Dust Impact on Solar Panels. *3D Research*, **10**, Article No. 214. <https://doi.org/10.1007/s13319-018-0214-7>
- [10] Mackey, E.A., Christopher, S.J., Lindstrom, R.M., Long, S.E., Marlow, A.F., Murphy, K.E. and Spatz, R.O. (2010) Certification of Three NIST Renewal Soil Standard Reference Materials for Element Content: SRM 2709a San Joaquin Soil, SRM 2710a Montana Soil I, and SRM 2711a Montana Soil II. NIST Special Publication 260-172, 1-39.
- [11] Nahar, N.M. and Gupta, J.P. (1990) Effect of Dust on Transmittance of Glazing Materials for Solar Collectors under Arid Zone Conditions of India. *Solar & Wind Technology*, **7**, 237-243. [https://doi.org/10.1016/0741-983X\(90\)90092-G](https://doi.org/10.1016/0741-983X(90)90092-G)
- [12] Hasan, A. and Sayigh, A. (1992) The Effect of Sand Dust Accumulation on the Light Transmittance, Reflectance, and Absorbance of the PV Glazing. In: *Renewable Energy, Technology and the Environment*, Pergamon Press, Oxford, 461-466.
- [13] Gürtürk, M., Benli, H. and Ertürk, N.K. (2018) Effects of Different Parameters on Energy-Exergy and Power Conversion Efficiency of PV Modules. *Renewable and Sustainable Energy Reviews*, **92**, 426-439. <https://doi.org/10.1016/j.rser.2018.04.117>
- [14] El-Shobokshy, M.S. and Hussein, F.M. (1993) Effect of the Dust with Different Physical Properties on the Performance of Photovoltaic Cells. *Solar Energy*, **51**, 505-511. [https://doi.org/10.1016/0038-092X\(93\)90135-B](https://doi.org/10.1016/0038-092X(93)90135-B)
- [15] Javed, W., Wubulikasimu, Y., Figgis, B. and Guo, B. (2017) Characterization of Dust Accumulated on Photovoltaic Panels in Doha, Qatar. *Solar Energy*, **142**, 123-135.

- <https://doi.org/10.1016/j.solener.2016.11.053>
- [16] Paudyal, B.R. and Shakya, S.R. (2016) Dust Accumulation Effects on Efficiency of Solar PV Modules for Off Grid Purpose: A Case Study of Kathmandu. *Solar Energy*, **135**, 103-110. <https://doi.org/10.1016/j.solener.2016.05.046>
- [17] Zarei, T. and Abdolzadeh, M. (2016) Optical and Thermal Modeling of a Tilted Photovoltaic Module with Sand Particles Settled on Its Front Surface. *Energy*, **95**, 51-66. <https://doi.org/10.1016/j.energy.2015.11.045>
- [18] Gu, J., Ramamoorthi, R., Belhumeur, P. and Nayar, S. (2007) Dirty Glass: Rendering Contamination on Transparent Surfaces. In: *Proceedings of the 18th Eurographics conference on Rendering Techniques*, Eurographics Association, Grenoble, France, 159-170.
- [19] Mani, M. and Pillai, R. (2010) Impact of Dust on Solar Photovoltaic (PV) Performance: Research Status, Challenges and Recommendations. *Renewable and Sustainable Energy Reviews*, **14**, 3124-3131. <https://doi.org/10.1016/j.rser.2010.07.065>
- [20] Hegazy, A.A. (2001) Effect of Dust Accumulation on Solar Transmittance through Glass Covers of Plate-Type Collectors. *Renewable Energy*, **22**, 525-540. [https://doi.org/10.1016/S0960-1481\(00\)00093-8](https://doi.org/10.1016/S0960-1481(00)00093-8)
- [21] Ndiaye, A., Kébé, C.M., Ndiaye, P.A., Charki, A., Kobi, A. and Sambou, V. (2013) Impact of Dust on the Photovoltaic (PV) Modules Characteristics after an Exposition Year in Sahelian Environment: The Case of Senegal. *International Journal of Physical Sciences*, **8**, 1166-1173.
- [22] Ansmann, A., Seifert, P., Tesche, M. and Wandinger, U. (2012) Profiling of Fine and Coarse Particle Mass: Case Studies of Saharan Dust and Eyjafjallajökull/Grimsvötn Volcanic Plumes. *Atmospheric Chemistry and Physics*, **12**, 9399-9415. <https://doi.org/10.5194/acp-12-9399-2012>
- [23] Rao, A., Pillai, R., Mani, M. and Ramamurthy, P. (2014) Influence of Dust Deposition on Photovoltaic Panel Performance. *Energy Procedia*, **54**, 690-700. <https://doi.org/10.1016/j.egypro.2014.07.310>
- [24] Saidan, M., Albaali, A.G., Alasis, E. and Kaldellis, J.K. (2016) Experimental Study on the Effect of Dust Deposition on Solar Photovoltaic Panels in Desert Environment. *Renewable Energy*, **92**, 499-505. <https://doi.org/10.1016/j.renene.2016.02.031>
- [25] Marticorena, B., Haywood, J., Coe, H., Formenti, P., Liousse, C., Mallet, M. and Pelon, J. (2011) Tropospheric Aerosols over West Africa: Highlights from the AMMA International Program. *Atmospheric Science Letters*, **12**, 19-23. <https://doi.org/10.1002/asl.322>
- [26] Lawrence, C.J. (1990) Spin Coating with Slow Evaporation. *Physics of Fluids A: Fluid Dynamics*, **2**, 453-456. <https://doi.org/10.1063/1.857823>
- [27] Pristiniski, D., Kozlovskaya, V. and Sukhishvili, S.A. (2006) Determination of Film Thickness and Refractive Index in One Measurement of Phase-Modulated Ellipsometry. *JOSA A. Journal of the Optical Society of America A*, **23**, 2639-2644. <https://doi.org/10.1364/JOSAA.23.002639>
- [28] Holben, B.N., Eck, T.F., Slutsker, I.A., Tanre, D., Buis, J.P., Setzer, A. and Lavenue, F. (1998) AERONET—A Federated Instrument Network and Data Archive for Aerosol Characterization. *Remote Sensing of Environment*, **66**, 1-16. [https://doi.org/10.1016/S0034-4257\(98\)00031-5](https://doi.org/10.1016/S0034-4257(98)00031-5)
- [29] Bashara, N.M. and Azzam, R.M. (1977) Ellipsometry and Polarized Light. NH, Amsterdam.
- [30] Mahdjoub, A., Moualkia, H., Remache, L. and Hafid, A. (2015) Analyse des spectres

- de transmittance des couches minces par une modélisation mathématique appropriée. *Revue Algérienne de Physique*, **2**, 30-37.
- [31] Berthier, S. and Lafait, J. (1981) Modélisation des propriétés optiques des milieux inhomogènes à structure complexe. *Le Journal de Physique Colloques*, **42**, 285-299. <https://doi.org/10.1051/jphyscol:1981119>
- [32] Macleod, H.A. and Macleod, H.A. (2010) *Thin-Film Optical Filters*. CRC Press, Boca Raton. <https://doi.org/10.1201/9781420073034>
- [33] Born, M. and Wolf, E. (2013) *Principles of Optics: Electromagnetic Theory of Propagation, Interference and Diffraction of Light*. Elsevier, Amsterdam.
- [34] McCrackin, F.L., Passaglia, E., Stromberg, R.R. and Steinberg, H.L. (1963) Measurement of the Thickness and Refractive Index of Very Thin Films and the Optical Properties of Surfaces by Ellipsometry. *Journal of Research of the National Bureau of Standards. Section A, Physics and Chemistry*, **67**, 363-377. <https://doi.org/10.6028/jres.067A.040>
- [35] Xie, L., Zhong, H., Du, Z. and Zhou, J. (2020) Monte Carlo Simulation of Electromagnetic Wave Transmittance in Charged Sand/Dust Storms. *Journal of Quantitative Spectroscopy and Radiative Transfer*, **241**, Article ID: 106744. <https://doi.org/10.1016/j.jqsrt.2019.106744>
- [36] Yun-Yun, Q. and Zhang, L.Z. (2017) Experimental Investigation of the Anti-Dust Effect of Transparent Hydrophobic Coatings Applied for Solar Cell Covering Glass. *Solar Energy Materials and Solar Cells*, **160**, 382-389. <https://doi.org/10.1016/j.solmat.2016.10.043>
- [37] Mastekbayeva, G.A. and Kumar, S. (2000) Effect of Dust on the Transmittance of Low Density Polyethylene Glazing in a Tropical Climate. *Solar Energy*, **68**, 135-141. [https://doi.org/10.1016/S0038-092X\(99\)00069-9](https://doi.org/10.1016/S0038-092X(99)00069-9)
- [38] Kaufman, Y.J., Tanré, D., Dubovik, O., Karnieli, A. and Remer, L.A. (2001) Absorption of Sunlight by Dust as Inferred from Satellite and Ground-Based Remote Sensing. *Geophysical Research Letters*, **28**, 1479-1482. <https://doi.org/10.1029/2000GL012647>
- [39] Müller, T., Schladitz, A., Massling, A., Kaaden, N., Kandler, K. and Wiedensohler, A. (2009) Spectral Absorption Coefficients and Imaginary Parts of Refractive Indices of Saharan Dust during SAMUM-1. *Tellus B: Chemical and Physical Meteorology*, **61**, 79-95. <https://doi.org/10.1111/j.1600-0889.2008.00399.x>
- [40] Said, S.A. and Walwil, H.M. (2014) Fundamental Studies on Dust Fouling Effects on PV Module Performance. *Solar Energy*, **107**, 328-337. <https://doi.org/10.1016/j.solener.2014.05.048>
- [41] Al-Hasan, A.Y. (1998) A New Correlation for Direct Beam Solar Radiation Received by Photovoltaic Panel with Sand Dust Accumulated on Its Surface. *Solar Energy*, **63**, 323-333. [https://doi.org/10.1016/S0038-092X\(98\)00060-7](https://doi.org/10.1016/S0038-092X(98)00060-7)
- [42] Ebert, D. and Bhushan, B. (2012) Transparent, Superhydrophobic, and Wear-Resistant Coatings on Glass and Polymer Substrates Using SiO<sub>2</sub>, ZnO, and ITO Nanoparticles. *Langmuir*, **28**, 11391-11399. <https://doi.org/10.1021/la301479c>
- [43] Duell, M., Ebert, M., Muller, M., Li, B., Koch, M., Christian, T. and Doble, D.M. (2010) Impact of Structured Glass on Light Transmission, Temperature and Power of PV Modules. *Proc. 25th European Photovoltaic Solar Energy Conf. and Exhibition*, Valencia, 3867-3872.
- [44] Chaouki, F., Anana, W., Laarabi, B., Sebbar, M.A., El Mahi, M., Barhdadi, A. and Boardman, J. (2016) Physical and Chemical Analysis of Outdoor Dust Deposited on

Photovoltaic Panels Installed in Rabat. 2016 *International Renewable and Sustainable Energy Conference (IRSEC)*, November 2016, 148-151.  
<https://doi.org/10.1109/IRSEC.2016.7983995>